A book chapter in **Mechanics and Reliability of Actuating Materials**, p. 273-291, Springer, 2005

Biofilm Growth: Perspectives on Two-Phase Mixture Flow and Fingerings Formation

S, Hao*[1], B. Moran*, D. Chopp**, B. Rittmann***
*Department of Mechanical Engineering
**Department of Engineering Science and Applied Mathematics
***Department of Civil and Environmental Engineering
Northwestern University, Evanston, IL 60208, U. S. A.

Abstract

The motion of biofilm in aqueous environment is modeled as two-phase mixture flow which is governed by a generalized Novier-Stokes equation. Noticed that the propagation of bacteria colonies obeys the diffusion law with the similar instability mechanism in the coarsening of metallic grains during solidification, a thermodynamic framework has been derived which reveals the two competing mechanisms in biofilm growth: (1) the absorption of nutrition from water phase that tends to maximize the contact area between biofilm and environment, which results in a fingering-like surface morphology; (2) the formation of a loose-surface layer that confines a biofilm to accommodate bacteria colonies, which tends to keep a sphere surface morphology so as to minimize system energy. An entropy-based condition has been obtained which quantitatively defines the effects of these two competing mechanisms on biofilm growth. One and two dimensional numerical simulations have been performed.

1. Introduction

A biofilm is an aggregation of microorganisms immobilized in an organic extracellular polymer matrix of microbial origin and anchored to biological or non-biological substrate surfaces in aqueous environment. This surface association is an efficient means of lingering for bacteria colonies in a favorable microenvironment, rather than being swept away by the current. Biofilm growth is the evolution and decay of such a self-organism organism system through the interiour and exterior cycles of energy exchange, representing the significant and incompletely understood mode of the propagation of bacteria in natural environment and during the distribution of infectious diseases which involves the interactions between ecological, biological, chemical and mechanical processes. Therefore, progresses in biofilm research will bring significant impacts to both modern industries and the daily life of human beings. This also provides challenges and opportunities for mechanical engineers to work with environmental engineers, microbiologists, and applied mathematicians in biofilm research. Reviews of recent development of biofilm can be found in [1-4].

Phenomenologically, biofilm growth is a mechanical process that couples diffusion, transportation, chemical reaction, and interaction between fluid and polymer-like soft substance (biofilm) with many underlying biological and ecological mechanisms. From the viewpoint of

[1] Corresponding author, suhao@northwestern.edu, suhao1@yahoo.com

continuum mechanics, the motion of biofilm can be modeled as the two-phase flow where the water phase can be assumed as incompressible flow while the biofilm phase is assumed as a viscous soft body governed by a generalized convection-diffusion equations, which will be discussed in details in this research. The biofilm phase contains two components: the bacteria cells that consists of one or several active species (bacterium families); and the biomass that consists of extracellular polymeric substances(EPS), primary biotic origin, such as the accumulation of dead cells [1, 2], and water. The active bacteria cells continuously emit small molecules that bear the information of the bacteria, which can be interpreted phenomenologically as "signals", to the environment; this process is termed "quorum sensing". When the concentrations of the signals and active cell density are over their threshold values, the signals interact with certain transcriptional regulators that modulate the expression of quorum sensing-regulated genes and cause drastic change in the rate of bacteria birth and death, which results in the mesoscopic size and shape of biofilm. This process is accomplished by the energy exchange through the consumption of the nutrition, termed "limiting growth substrates", from the water phase [1, 2]. Fig. 1 illustrates this life cycle of bacteria in biofilm, which is the dominant mechanism in the mechanical system introduced in this analysis.

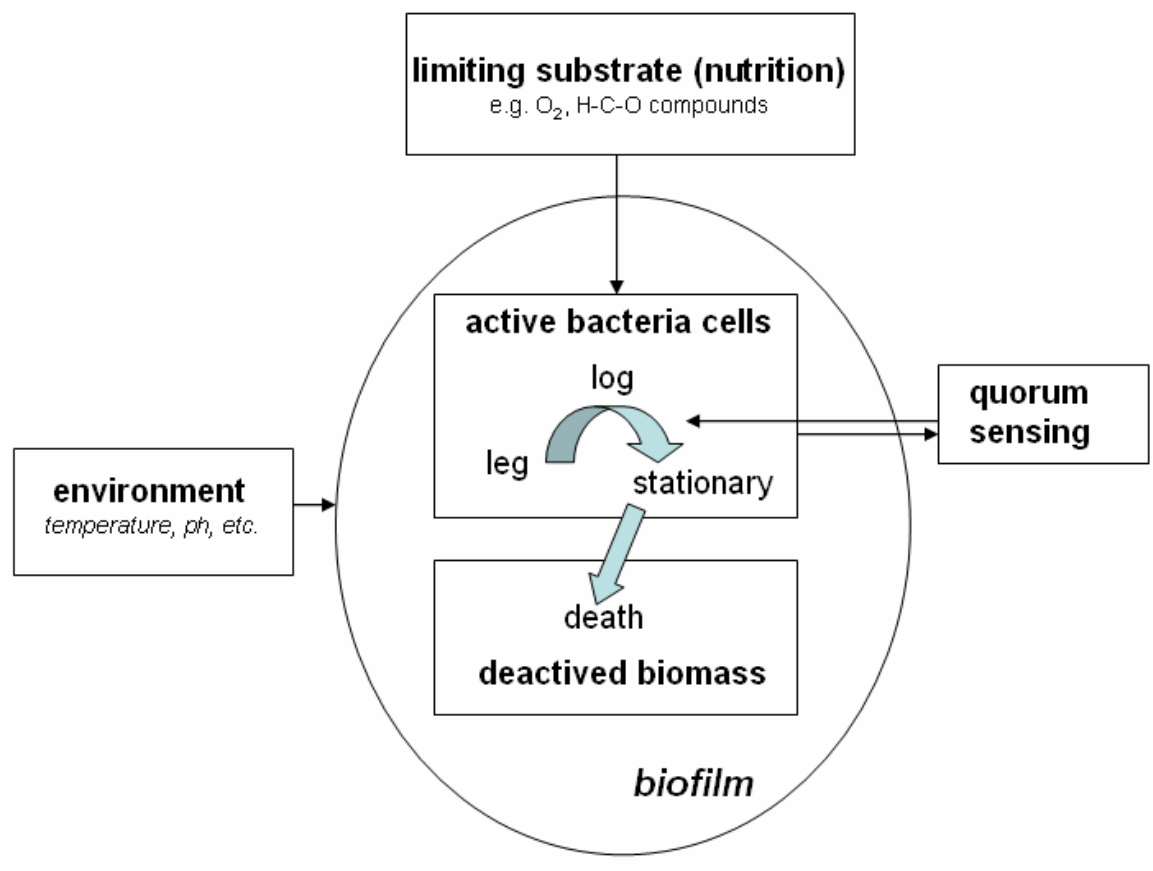

Fig. 1 Life cycle of bacteria in biofilm in aqueous environment

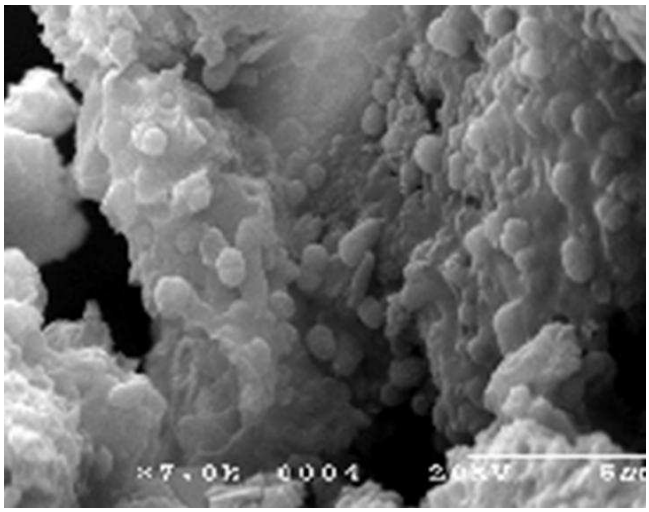

Fig. 2 Finger-shaped biofilm

Therefore, in the framework of continuum mechanics, the dynamics of biofilm growth can be characterized by the evolution of the interface between biofilm and water phase through the advection-diffusion field solution of the three key-biological variables: total living cells mass concentration m_b, the limiting growth substrate concentration m_O, and the quorum sensing concentration m_a. As compared to other fluid-solid interaction problems, an interesting and important feature of biofilm is its heterogenenuous nature that contains the cycle of deaths and creatures of bacterium through the diffusion-consumption of the limiting substrate absorbed from water phase.

Observations reveal that the propagation of biofilm sometimes presents a finger-shaped interface to the water phase (Fig. 2). This morphology is a nature selection from environment which provides optimized inhabitable condition for a certain group of bacteria inhabitants, thus, it governs the evolution and decay for this class of biofilms. While considerable studies have been reported in the respects of microbiology, ecology, and physiology, it seems that relatively little attention has been paid to the bio-mechanical functions and responses for such a fingering morphology and underlying physics in biofilm growth. In a two-phase mixture flow, the outer profile of the biofilm defines the boundary condition for a boundary value problem of biofilm phase and, thus, determines the underlying mechanical processes such as sloughing, detachment, bacteria cells loss and growth. In recent years, an increasing interesting can be found in mathematic and mechanical modeling and simulation [2, 5-7]. Among them, Dockery and Klapper studied the biofilm fingering formation [5]. In their paper this phenomenon is treated mathematically as a loss of stability of a growing biofilm outer profile due to the hydrostatic pressure from water phase.

The finger-like morphology can be found in many diffusion-convection systems in nature, among which the alloys precipitate, solidification, and coarsening is a well-known process with dendritic moving boundary that has been thoroughly investigated in materials science[8, 9]. In this study, a model applying the diffusion instability theory in metallurgical analysis has been proposed to describe a fingering-shaped biofilm growth in the framework of a generalized

Navier-Stokes equation. As verification, numerical simulations have also been performed. Hereafter both the terminologies "dentritic" and "finger-like" refer to the same waived morphology of biofilm surface.

This paper is organized as follows: The next section gives the derivation of a generalized Navies-Stocks equation with a brief introduction of biofilm evolution equation. The section III presents the proposed model of the dendritic biofilm propagation. Examples of numerical simulation using proposed model and discussions are given in the section IV. The conclusions are given in the section V.

In this paper boldface symbols denote tensors, the order of which is indicated by the context. Plain symbols denote scalars or a component of a tensor when subscript-indices are attached. Repeated indices are summed. For two order tensors **a** and **b**: $\mathbf{a} = \lfloor a_{ij} \rfloor$, $\mathbf{b} = \lfloor b_{ij} \rfloor$: $\mathbf{a} \cdot \mathbf{b} = \lfloor a_{ik} b_{kj} \rfloor$, $\mathbf{a} : \mathbf{b} = \lfloor a_{ij} b_{ij} \rfloor$, and $\mathbf{ab} = \lfloor a_{ij} b_{kl} \rfloor$. The symbol ∇ represents the gradient operator: $\nabla = \lfloor \partial / \partial_i \rfloor$; and $\nabla^2 = \nabla \cdot \nabla$.

2. A Model of Biofilm Growth and Governing Equations

2.1 A Generalized "Navier-Stokes Equation"

As illustrated in Fig. 3a, a biofilm growth is modeled as a two-phase mixture flow coupling diffusion and reaction where the latter represents the life cycle of bacteria cells without inquiring into its biologic basis. In the biofilm model of Fig. 3b a region ($\Omega \subset R^2$) is divided into a biofilm region Ω_b and an aqueous region Ω_w with the interface surface Γ_b. We use the subscript '*w*', '*O*', '*a*', 'EPS', and '*k*', respectively, to denote in turn the variables associated with the liquid water (H_2O), limiting substrate(O_2), signal of quorum sensing, extracellular polymeric substances(*EPS*), and the k^{th} specie of bacterium in biofilm; when totally *n* species of bacteria exist, then $k = 1,2,,...,n$.

Let 'm_i' to be the mess of the i^{th} component per unit volume in a multi-phase system and 'f_i' to be its volume fraction; e.g. 'm_{EPS}' is the mass of *EPS* per unite volume, 'f_{EPS}' is the volume fraction of *EPS*, and 'm_{total}' is the total mess per unit volume; then, for a boundary value problem defined in Fig.3b with *n* species of bacteria:

$$m_W + m_O + m_a + m_{EPS} + \sum_{k=1}^{n} m_k = m_{total} \tag{2.1a}$$

and

$$f_W + f_O + f_a + f_{EPS} + \sum_{k=1}^{n} f_k = 1 \tag{2.1b}$$

Next, let '$\overline{\rho}_i$' to be the density of pure i^{th} component per unit volume and 'ρ_i' to be the density of i^{th} component per unit volume in a multi-phase system, respectively:

$$f_i \overline{\rho}_i = m_i = \rho_i$$

Therefore, 'm_i' is the "density fraction" of the i^{th} specie in the multi-phase system.

Hence, the mass concentrations of each bacterium specie, together with the velocity field $\boldsymbol{v} = [v_i]$, total mess per unit volume m_{total}, and the energy per unit volume 'e', are the $n+9$ governing variables that define the boundary value problem of biofilm growth.

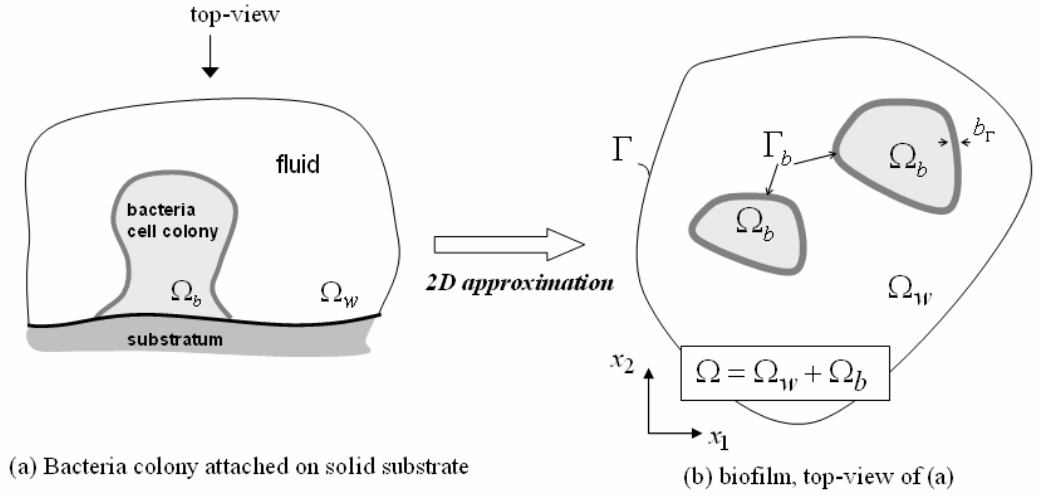

Fig. 3 An illustration of the analyzed problem

Alternatively, using the subscripts 'b' and 'd' to denote the active bacteria cells and deactivated biomass, respectively; then in Ω_b we have

$$m_b = \sum_{k=1}^{n} m_k \qquad \text{and} \qquad m_d = m_{EPS} \tag{2.2}$$

For this boundary value problem of biofilm growth, the following approximations are employed

(1) incompressible flow
(2) isothermal process
(3) the interface surface Γ_b is defined by m_{cr}, a critical value for the total concentration of the active bacteria cells and deactivated biomass

$$m_{cr} = [m_b]_{\Gamma_b} \tag{2.3}$$

(4) a boundary layer enhanced to Γ_b exists within biofilm phase; which has a constant thickness b_Γ and is associated with an extra additional surface energy density $\chi(\boldsymbol{x})$.

We consider the problem in a Eularian coordinate system $\{\boldsymbol{x}\}$ and begin with the diffusion problem of a field variable $\phi(\boldsymbol{x})$ which is characterized by the flux field $\boldsymbol{j}_\phi$ that is proportional to the gradient of ϕ (Fick's law):

$$\boldsymbol{j}_\phi = -B_\phi \nabla \phi \tag{2.4}$$

where B_ϕ is diffusion coefficient. When there is no transportation, the difference between the reaction rate $q_\phi(\boldsymbol{x})$ of ϕ at $\boldsymbol{x}$ and the divergence of $\boldsymbol{j}_\phi$ represents the rate of net change of ϕ at this point:

$$\dot{\phi} = q_\phi - \nabla \cdot \boldsymbol{j}_\phi \tag{2.5}$$

In an aqueous environment characterized by the flow velocity field $\boldsymbol{v}$, the net change of ϕ at the spatial point **x** is the summation of the change of ϕ itself and the transportation due to the flow, expressed as $\nabla \cdot (\phi \boldsymbol{v})$:

$$\dot{\phi} = \phi_{,t} + \nabla \cdot (\phi \boldsymbol{v}) \qquad \text{i.e.} \qquad \frac{d\phi(\boldsymbol{x},t)}{dt} = \frac{\partial \phi}{\partial t} + \nabla \cdot (\phi \boldsymbol{v}) \tag{2.6}$$

Substituting (2.4) and (2.6) into (2.5), the latter becomes:

$$\phi_{,t} = -\nabla \cdot (\phi \boldsymbol{v}) + B_\phi \nabla^2 \phi + q_\phi \tag{2.7}$$

or, alternatively

$$\phi_{,t} + \nabla(\phi \boldsymbol{v}) - B_\phi \nabla^2 \phi - q_\phi = 0 \tag{2.8}$$

In (2.7) and (2.8) B_ϕ, the diffusion coefficient, is assumed to be a constant

Remarks:

1) When $\phi = \rho$, the total density, so $q_\rho = 0$ and (2.8) becomes the conventional "mass conservation law".

2) Considering Newtonian flow so $\phi = \rho \boldsymbol{v}$ and $q_\phi = \rho \bar{\boldsymbol{f}}$, where $\bar{\boldsymbol{f}}$ is the body force vector, the correspondent constitutive relation is:

$$\boldsymbol{\sigma} = \boldsymbol{C}(C_\mu, C_\kappa) : \boldsymbol{d} - \boldsymbol{I} p_0 \qquad \text{and} \qquad \boldsymbol{d} = \lfloor d_{ij} \rfloor, \qquad d_{ij} = \frac{1}{2}(v_{i,j} + v_{j,i}) \tag{2.9}$$

where $\boldsymbol{\sigma}$ is stress tensor, $\boldsymbol{C}$ is the stiffness matrix which is the function of shear viscosity coefficient C_μ and bulk modulus C_κ, $\boldsymbol{I}$ is the two order unit tensor and p_0 is the initial hydrostatic pressure. Then (2.8) becomes the "momentum conservation law" in conventional fluid dynamic.

3)When $\phi = \rho e$ and $q_\phi = q_H$, the heat source per unit mass, then (2.8) degenerates to the energy conservation law; where e is the total energy per unit mass in either water phase or biofilm phase:

$$e = \varphi_{el} + RC_p T + \frac{1}{2} v_i v_i \tag{2.10}$$

where φ_{el} is the elastic energy; T is absolute temperature, C_p is isothermal heat capacity, R is universal gas constant; the product of RC_pT represents the intrinsic energy of unit mass in the

system. Alternatively, φ_{el} is also termed as"energy potential" and the product RC_iT is considered as the internal energy per unit mass.

4) The above mentioned five partial differential equations (mass conservation, momentum conservation, and energy conservation) are the conventional Navier-Stokes equations. More details of fluid dynamics can be found, e.g. in [10].

For the biofilm problem, (2.8) can be rewritten in a general form:

$$\boldsymbol{\varphi}_{,t} + \nabla \cdot (\boldsymbol{v}\,\boldsymbol{\varphi}) - \nabla \cdot (\boldsymbol{B} \cdot \nabla \boldsymbol{\varphi}) - \boldsymbol{Q} = 0 \tag{2.11}$$

where $\boldsymbol{\varphi} = [m_W, m_O, m_a, m_{EPS}, m_1, m_2, ..., m_n, \rho, e, \boldsymbol{v}]$ with totally $n+9$ components (n+8 components for two-dimensional case), $\boldsymbol{B}$ is a matrix that contains the system stiffness and diffusion coefficients; where the stiffness is determined by (2.9) and the diffusion coefficients can be found, e.g., in [1, 2]. In this analysis three different constant diffusion coefficients of biomass are engaged, corresponding to the diffusion in water phase, surface layer, and biofilm phase. In (2.11) $\boldsymbol{Q}$ is the reaction vector corresponding to each term of $\boldsymbol{\varphi}$, $\boldsymbol{Q} = \{q_i\}$; in which q_i is the source of ϕ_i, the i^{th} component of $\boldsymbol{\varphi}$. It can be expressed as

$$q_i = \sum_{k=1}^{N_i} \Lambda_{ik}\, j_k \tag{2.12}$$

where N_i is the number of reactions involved for ϕ_i; j_k is the rate of the k^{th} reaction and Λ_{ik} is the corresponding "mass stoichiometric coefficient". The detail expresses of j_k and Λ_{ik} will be discussed at the next subsection.

In this paper the partial differential equations (2.11) is termed as the "generalized Navier-Stokes equation" for the two-phase mixture flow with biofilm.

2.2 Biofilm kinetics – evolution equations

As an organic system, the evolution and decay of biofilm are the life cycles of bacteria involving the following four major energy exchange and transformations processes [11]:

(1) creation (new born) of bacteria population through the absorption of the nutrition, i.e. the "limiting substrate"; the heredity and variation of the bacteria are governed by synthase signals represented by the signals concentration "m_a";

(2) quorum sensing: creation and emission of the synthase signals;

(3) death of bacteria that creates inert biomass to be a part of the extracellular polymeric substances (EPS);

(4) inorganic chemical reactions in the EPS and water, such as the biodegradation of the inert biomass.

The correspond mathematic expression of the reaction rates have been studied in [2] which are applied in this research. For the case of single bacterium specie ($n=1$) without heat source ($q_H=0$), so $\boldsymbol{Q} = [0, q_O, q_a, q_{EPS}, q_b, 0, 0, 0, 0, 0]$ and the corresponding coefficients are listed in the table I:

Table I The mass stoichiometric coefficients and reaction rates [2]

	q_b	q_a	q_{EPS}	q_O
N_i	2	3	2	2
Λ_{i1}	m_b	m_b	$0.2m_b$	m_b
j_1	$Y_{X/O}\hat{q}_0 \cdot \mu(m_O, K_0)$	$\beta_1 \cdot \mu(m_O, K_0)$	$b \cdot \mu(m_O, K_0)$	$-\hat{q}_0 \cdot \mu(m_O, K_0)$
Λ_{i2}	m_b	m_b	m_b	$0.8m_b$
J_2	$-b \cdot \mu(m_O, K_0)$	β_3	$Y_{W/O}\hat{q}_0 \cdot \mu(m_O, K_0)$	$-b\hat{\gamma} \cdot \mu(m_O, K_0)$
Λ_{i3}		m_b		
J_3		$\beta_2 H(m_b + m_d - m_{cr})$		

where K_O is the "half-maximum-rate concentration" for utilization of substrate; $Y_{x/O}$, $\hat{q}_O$, b, and $\hat{\gamma}$ are the constants termed as "yield of active biomass", "maximum specific substrate utilization rate", "rate of endogenous decay", and "chemical oxygen demand" for the degradation of a unit of active biomass; β_1 and β_3 are the coefficients of basal rate of signal production whereas β_2 is the coefficient for the additional quorum sensing represented by the Heaviside function

$$H(x) = \begin{cases} 1 & x \geq 0 \\ 0 & x < 0 \end{cases} \tag{2.13}$$

Also in table I the $\mu(x, K_0)$ denotes the Monod kinetic:

$$\mu(x, K_0) = \frac{x}{K_O + x} \tag{2.14}$$

2.3 Initial Condition and boundary conditions

For any variable ϕ_i in (2.11) the initial condition is:

$$\text{at } t = t_0: \quad \phi_i = \phi_{i0} \quad \text{where} \quad \phi_{i0} = \phi_i(\boldsymbol{x}, t_0) \ \forall \mathbf{x} \in \Omega \tag{2.15}$$

Particularly, for the hydrodynamic pressure *p*:

$$\text{at } t = t_0: \quad p = p_0 \quad \text{otherwise} \quad p = -C_\kappa \dot{\varepsilon}_{ii} + p_0 \tag{2.16}$$

Hence, for incompressible flow:

$$\dot{\varepsilon}_{ii} \equiv 0 \quad \text{so} \quad p \equiv p_0 \tag{2.17}$$

Boundary conditions on Γ in Fig. 3 are:

$$\phi_i\big|_\Gamma = \bar{\phi}_i \quad \text{or} \quad \boldsymbol{n} \cdot \nabla \phi_i = \bar{\boldsymbol{J}}_i \tag{2.18}$$

where $\bar{\boldsymbol{J}}_i$ is the flux on Γ for ϕ_i.

2.4 Lever-Set representation of the interface Γ_b

Let the density concentration of active bacteria:

$$\psi(\boldsymbol{x}) = m_b(\boldsymbol{x}) \tag{2.19}$$

to be a lever-Set function, so Γ_b, the interface between biofilm and water phase, can be represented as following:

$$\frac{\partial \psi}{\partial t} + F|\nabla \psi| = 0; \qquad F = \frac{\nabla \psi}{|\nabla \psi|} \cdot \boldsymbol{u}_{\Gamma_b} \tag{2.20}$$

where $\mathbf{u}_{\Gamma_b}$ is the velocity vector of Γ_b when $\psi(\mathbf{x}) = m_{cr}$.

2.5 Kinetic of biofilm growth – evolution of interface Γ_b

Let v_{Γ_b} to be the velocity of the interface Γ_b along $\boldsymbol{n}_{\Gamma_b}$, the unit vector along the outer normal direction of Γ_b during biofilm growth, by employing the Fick's law (2.4) to the $m_b(\boldsymbol{x})$ and substituting the criterion (2.3), the left hand side of (2.4), i.e. the flux of $m_b(\boldsymbol{x})$, reads:

$$\boldsymbol{j}_b = m_{cr} v_{\Gamma b} = m_{cr} \frac{\Delta u_{\Gamma_b}}{\Delta t} \tag{2.21a}$$

where Δu_{Γ_b} is the displacement of biofilm surface during time interval Δt. Then (2.4) becomes:

$$v_{\Gamma_b} = -\frac{B_b^{\chi}}{m_{cr}} \left[\boldsymbol{n}_{\Gamma_b} \cdot \nabla m_b \right] \qquad \text{or} \qquad \Delta u_{\Gamma_b} = -\frac{\Delta t B_b^{\chi}}{m_{cr}} \left[\boldsymbol{n}_{\Gamma_b} \cdot \nabla m_b \right] \tag{2.21}$$

where B_b^{χ} is the diffusion coefficient of $m_b(\boldsymbol{x})$ within the boundary layer enhanced to Γ_b. (2.21) represents a local form of the interface kinetic during biofilm growth

Integrating (2.21) along the entire interface Γ_b and applying (2.3), the left hand side of (2.21) becomes:

$$\oint_{\Gamma_b} v_{\Gamma_b} d\Gamma_b = \bar{v}_{\Gamma_b} S_b; \tag{2.22}$$

where $\bar{v}_{\Gamma_b}$ is the average velocity of Γ_b during biofilm expansion and S_b is the area of biofilm surface:

$$\oint_{\Gamma_b} d\Gamma_b = S_b$$

Applying the Gaussian's integration theorem

$$\int_{\Omega_b} \nabla \cdot (a \nabla b) d\Omega = \oint_{\Gamma_b} (a \nabla b) \cdot \boldsymbol{n} d\Gamma_b \tag{2.23}$$

to the integration of the right hand side of (2.21) and substituting (2.11) into the resulted relation:

$$-\oint_{\Gamma_b}\frac{B_b^{\chi}}{m_{cr}}\left[\boldsymbol{n}_{\Gamma_b}\cdot\nabla m_b\right]d\Gamma_b=-\frac{1}{m_{cr}}\int_{\Omega_b}\nabla\left(B_b^{\chi}\nabla m_b\right)d\Omega_b=\frac{B_b^{\chi}}{m_{cr}}\int_{\Omega_b}\left(q_b-\dot{m}_b\right)d\Omega_b \tag{2.24}$$

According to the analysis in [2], $\dot{m}_b\approx 0$ within Ω_b, so the global form of the interface kinetic during biofilm growth is

$$\bar{v}_{\Gamma_b}=\frac{B_b^{\chi}}{m_{cr}S_b}\int_{\Omega_b}q_b d\Omega_b \qquad \text{or} \qquad \Delta\bar{u}_{\Gamma_b}=\frac{\Delta t B_b^{\chi}}{m_{cr}S_b}\int_{\Omega_b}q_b d\Omega_b \tag{2.25}$$

3. Thermodynamic Framework and Application to Fingering Formation

In this section we revisit the mass and energy conservations in biofilm with the reactions introduced by table I. A thermodynamic framework will be established which determines the dynamics and kinetics of biofilm growth.

3.1 Mass conservation for biofilm reaction

By superposition of the equations in (2.11) for $\boldsymbol{\varphi}=\left[m_w,m_O,m_a,m_{EPS},m_1,m_2,...,m_n\right]$, we obtain the conventional mass conservation law: $\rho_{,t}+\nabla\cdot(\boldsymbol{v}\,\rho)=0$ which leads to an additional constraint to the reaction rates:

$$\sum_{i=1}^{n+9}q_i=\sum_{i=1}^{n+9}\sum_{k=1}^{N_i}\Lambda_{ik}j_k=0 \tag{3.1}$$

This relation implies that mass can neither be created nor dismissed through chemical reactions, so there is at least one coefficient among those listed in Table I is predetermined by (3.1).

3.2 Rate of entropy production

The second thermodynamic law is the fundamental law that governs any nature process including biofilm growth. Let $s(\boldsymbol{x})$ to be the entropy function, the local form of the second thermodynamic law is:

$$\Delta s\geq 0 \tag{3.2}$$

According to Gibbs' equation the rate of entropy change is expressed as:

$$\lim_{\Delta t\to 0}\left[\rho\frac{\Delta s}{\Delta t}\right]=\frac{\rho}{T}\dot{u}+\frac{p}{T}\nabla\cdot\boldsymbol{v}-\frac{\rho}{T}\sum_k\eta_k\dot{m}_k \tag{3.3}$$

where p, T, and η_k are pressure, temperature, and the chemical potential for the k^{th} specie, respectively; u is the internal energy per unit mass that is defined as below in this study:

$$u(\boldsymbol{x}) = e(\boldsymbol{x}) + \chi(\boldsymbol{x}) - \Phi(\boldsymbol{x}) - \frac{1}{2}\boldsymbol{v}\cdot\boldsymbol{v} \tag{3.4}$$

where $\chi(\boldsymbol{x})$ is the interfacial energy per unit mass when $\boldsymbol{x}$ is within the surface layer enhanced to Γ_b; Φ is the summation of the potential energy for each component that defines the general force field $\boldsymbol{f}_k$:

$$\Phi = \sum_k m_k \Phi_k \qquad \text{and} \qquad \boldsymbol{f}_k = -\nabla\Phi_k \tag{3.5}$$

By substituting (3.4) and (3.5) into the conservation of energy in (2.11), we obtain

$$\rho\dot{u} = \rho\dot{\chi} - \nabla\cdot(\nabla T) - \boldsymbol{\sigma} : \nabla\boldsymbol{v} \qquad \text{here} \quad \dot{u} = \frac{du}{dt}, \quad \dot{\chi} = \frac{d\chi}{dt} \tag{3.6}$$

In the derivation of (3.6), several additional relations are applied which is listed in Appendix I. The chemical potential for ideal solution is employed in (3.3):

$$\eta_k = G_k + RT\log(m_k) \qquad \text{and} \qquad G_k = H_k - s_k T \tag{3.7}$$

where G_k, s_k, and H_k are the Gibbs free energy, entropy, and enthalpy for the k^{th} component of the system, respectively. The physical meaning of enthalpy is the chemical bonding energy of molecule. The Gibbs free energy for many biological C-H-O compounds are given in [1].

By substituting into (3.4-3.7) into (3.3) then (3.2) and applying (2.11), we obtain the "Clausius-Duheim" equation of the biofilm system, i.e. the local form of the second thermodynamic law:

$$\dot{s} = \frac{1}{T}\nabla\cdot(\nabla T) - \frac{1}{T}\boldsymbol{\sigma} : \nabla\boldsymbol{v} + \frac{p}{T}\nabla\cdot\boldsymbol{v} + \frac{\rho}{T}\dot{\chi} - \frac{\rho}{T}\sum_k \eta_k\left\{\nabla\cdot(B_k\nabla m_k) + \sum_{r=1}^{N_k}\Lambda_{kr}j_r\right\} \geq 0 \tag{3.8}$$

where B_k is the diffusion coefficient for m_k. In (3.8) the first term refers to the entropy change caused by heat flow; the following terms denote in turn the changes of visco-elastic strain energy, volumetric strain energy, interfacial energy, diffusion induced entropy and reaction induced entropy.

4. Finger-Shaped Biofilm Formation and Diffusion Instability

Experimental observations reveal that biofilm usually has a thick coherent surface layer over the film body that consists of semi-contiguous organisms unit, e.g. particles made of EPS and bacteria cells, and water channels [12, 13]. As the "frontier" to "fresh" water, the biological

function of the surface layer is to extract more limiting substrate, mainly O_2, to supply the nutrition for the film body. From the viewpoint of continuum mechanics, this surface layer is a nature shield that confines a favorable internal environment for the bacteria life cycle meanwhile prevents the semi-contiguous organisms to be sloughed or washed out. To form such a surface layer requires extra bonding energy to make the layer to be relatively coherent as compared to the inside part. This extra energy defines the function $\chi(\boldsymbol{x})$ that is introduced in (3.5).

We propose the two competing mechanisms which may govern the evolution of interfacial surface Γ_b. Since growth of biofilm is a bacteria population increase that results in volumetric enlargement of active biomass, this process requires the supply of nutrition from fresh water which tends to maximize its surface area, so as to absorb more limiting substrate. On the other hand, to maintain a stationary state, the energy equilibrium requires the system to minimize its surface because the latter requires extra coherent energy. The consumption of entropy, stated by the second thermodynamic law, adjusts the system under a balance between these two mechanisms and, thus, determines the surface morphology.

To quantitatively describe these two competing mechanisms, a biofilm surface evolution model is proposed which is illustrated in Fig. 4. In this diagram three pieces of biofilm are plotted which have the same interior area but different shapes of interfacial surface boundary. The circler biofilm (b) has the smallest boundary length, whereas the elliptic (a) and the qua-poles biofilms can be considered as waved boundaries with the first and third order frequencies, respectively. Then the problem can be addressed as: finding entropy consumption for the transformation from (b) to (a) or (b) to (c) or verse versa; the signs of the entropy consumption in these transformations determine the favorable morphology of the biofilm.

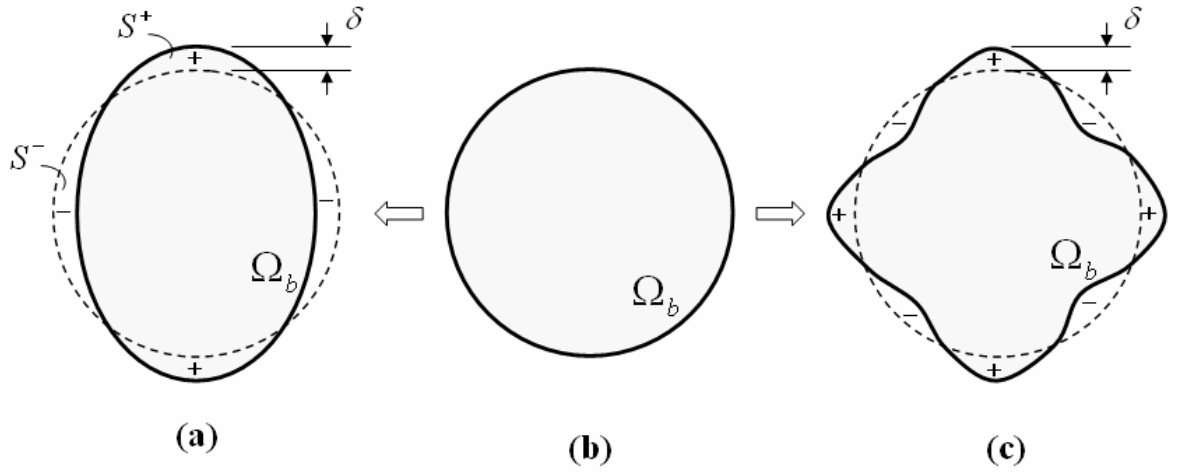

Fig. 4 A model for analyzing finger formation.

For simplification, we consider the case of $(\mathrm{b}) \Leftrightarrow (\mathrm{a})$ for the biofilm with single bacterium specie ($n=1$) with the following approximations:

A1: isothermal process, i.e. $T = \text{const}$;

A2: diffusion process dominates, so the convection terms can be omitted, i.e. $\boldsymbol{v} \cong \boldsymbol{0}$;

A3: no bacteria cell penetrating the biofilm boundary ($\nabla m_b\big|_{\Gamma_b} = 0$) and the creation of

bacteria only resulting in the expansion of biofilm;

A4: constant diffusion coefficients in (2.11);

A5: continuities for all variables of φ on and inside of Γ_b;

A6: the product of quorum sending signal is small, i.e. $\left[m_a << m_O\right]_{\Gamma_b}$ and $\left[\nabla m_a << \nabla m_O\right]_{\Gamma_b}$;

A7: axial symmetric distributions for all variables of φ in the case (b) of Fig. 4.

According to the approximations **A1, A2, A4,** and **A6**, the entropy change of the biofilm, represented by the integration of (3.8) over the biofilm domain in Fig. 4, becomes

$$\lim_{\Delta t\to 0}\int_{\Omega_b}\frac{\Delta s}{\Delta t}d\Omega = -\frac{\rho}{T}\int_{\Omega_b}\left[B_O\eta_O\nabla^2 m_O + B_b\eta_b\nabla^2 m_b - \dot{\chi} + \sum_{k=O,b}\eta_k q_k\right]d\Omega \ge 0 \tag{4.1}$$

where B_O and B_b are diffusion coefficients. Applying the following relations

$$a\nabla^2 b = \nabla\cdot(a\nabla b) - \nabla a\cdot\nabla b\,,\quad \int_{\Omega_b}\nabla\cdot(a\nabla b)d\Omega = \oint_{\Gamma_b}(a\nabla b)\cdot\boldsymbol{n}d\Gamma_b\,,\qquad \text{and}\qquad \nabla m_O = \boldsymbol{J}_O$$

, where $\boldsymbol{n}$ is the unit outer normal vector of Γ_b, then (4.1) can be rewritten in the form as

$$\lim_{\Delta t\to 0}\int_{\Omega_b}\frac{\Delta s}{\Delta t}d\Omega = -\frac{\rho}{T}\oint_{\Gamma_b}(B_O\eta_O\boldsymbol{J}_O)\cdot\boldsymbol{n}_{\Gamma_b}d\Gamma_b - \frac{\rho}{T}\int_{\Omega_b}\left[\dot{\tilde{s}} - \dot{\chi}\right]d\Omega \ge 0 \tag{4.2}$$

where the approximation **A7** ($\nabla m_b\big|_{\Gamma_b} = 0$) is also applied. In (4.2) the first term represents the nutrition (limiting substrate) that flows into the Ω_b under the chemical potential η_O; whereas $\dot{\tilde{s}}$ is the summation of the following terms

$$\dot{\tilde{s}} = \sum_{k=O,b}\eta_k q_k - B_O\nabla\eta_O\nabla m_O - B_b\nabla\eta_b\nabla m_b \tag{4.3}$$

For the transformation, e.g. $(\mathrm{b})\Rightarrow(\mathrm{a})$, the entropy rate can be expressed as the difference below:

$$\left[\int_{\Omega_b}\Delta s d\Omega\right]_{(b)\to(a)} = \Delta t\left[\int_{\Omega_b}\frac{\Delta s}{\Delta t}d\Omega\right]_{(b)} - \Delta t\left[\int_{\Omega_b}\frac{\Delta s}{\Delta t}d\Omega\right]_{(a)} \tag{4.4}$$

Keeping in mind that no changes in area and substituting (4.2) into (4.4), so the difference for the first term of (4.2) is

$$-\left[\oint_{\Gamma_b}(B_O\eta_O\boldsymbol{J}_O)\cdot\boldsymbol{n}_{\Gamma_b}d\Gamma_b\right]_{(b)} + \left[\oint_{\Gamma_b}(B_O\eta_O\boldsymbol{J}_O)\cdot\boldsymbol{n}_{\Gamma_b}d\Gamma_b\right]_{(a)} = B_O\eta_{O\Gamma}\left|\boldsymbol{J}_{O\Gamma}\right|\Delta\Gamma_b + o(\Delta\Gamma_b) \tag{4.5}$$

where $\eta_{O\Gamma}$ and $\boldsymbol{J}_{O\Gamma}$ are the η_O and $\boldsymbol{J}_O$ on Γ_b for the case (b) in Fig. 4. Hence, (4.5) represents the increment of nutrition flow due to the length increment of surface layer when (b) shifts to (a) (or (c)). Consequently, there should be also a correspondent term for the increment of surface energy:

$$-\int_{\Omega_b}[-\dot{\chi}]_{(b)}d\Omega+\int_{\Omega_b}[-\dot{\chi}]_{(a)}d\Omega=\frac{\Delta\chi}{\Delta t}\Delta\Gamma_b b_\Gamma+o(\Delta\Gamma_b) \tag{4.6}$$

where b_Γ is the thickness of the boundary layer enhanced to Γ_b. By the elementary calculation detailed in Appendix II, we know that the rest terms in (4.4) are in the order of $o(\Delta\Gamma_b)$. When the δ in case (a) and (c) of Fig. 4 is a small perturbation parameter, then $\Delta\Gamma_b$ is also a small quantity.

Finally, by leaving out the terms in the order of $o(\Delta\Gamma_b)$ and taking Δt to be unit, the (4.4) becomes:

$$\lim_{b\to a}\int_{\Omega_b}\Delta s d\Omega=B_O\eta_{O\Gamma}|\boldsymbol{J}_{O\Gamma}|\Delta\Gamma_b-\chi b_\Gamma\Delta\Gamma_b\geq 0 \tag{4.7}$$

The underlying physics of (4.7) can be explained through two extreme cases: when the surface coherent energy density is infinitesimal or vanishes, i.e. $\chi\Rightarrow 0$ and the biofilm is the simply aggregation of bacteria cells and deactivated biomass without surface coherence, so

$$\lim_{b\to a}\int_{\Omega_b}\Delta s d\Omega=B_O\eta_{O\Gamma}|\boldsymbol{J}_{O\Gamma}|\Delta\Gamma_b\geq 0 \tag{4.8}$$

which implies that a fingering shape formation, which increases $\Delta\Gamma_b$, is a thermodynamically favorable motion during the biofilm growth. On the other hand, when $\chi\neq 0$ and $b_\Gamma\chi >> B_O\eta_{O\Gamma}|\boldsymbol{J}_{O\Gamma}|$, i.e., the biofilm has a well coherent surface, then (4.7) becomes:

$$\lim_{b\to a}\int_{\Omega_b}\Delta s d\Omega\approx-\chi b_\Gamma\Delta\Gamma_b\geq 0 \tag{4.9}$$

To ensure that the greater or equal sign holds in (4.9), $\Delta\Gamma_b$ must vanish; i.e. the biofilm intends to keep a spherical shape.

Hence, the surface morphology of biofilm is determined by the amplitude of the surface layer coherence energy density. When a biofilm is an aggregation of loosely contiguous particle with minimized surface coherence, then according (4.8) a finger-typed surface is a preferred morphology. Whereas for a biofilm that has a well-formed coherent surface layer, the smooth spherical surface is the preferred morphology. This phenomenon is essential the same as the

metal grain solidification during cooling process where the melted metal tends to maximized the surface area of the precipitated solid colonies so as to promote heat conduct whereas the capillary force tends to minimize the surface area so as to minimize system energy. This metallurgical process has been thoroughly investigated in [8, 9, 14].

5. Numerical Example

Simulation of growing "Pseudomonas aeruginosa" biofilm has been performed using a LEM technique (Level Set {Sethian, 1999 #340} based on E-FEM enrichment{Belytschko, 1999 #177} + MPFEM{Hao, 2003 #315}), where the interface surface between biofilm and water phase is represented by level set function (2.19-2.20); the simulation accuracy is secured by applying the enrichment technique from E-FEM with minimum remeshing; the Moving Particle Finite Element (MPFEM) is used to avoid the effects of mesh distortion. Standard Galerkin solution procedure for diffusion problems is applied; however, an additional panelty term representing (4.8) has been added into the weak form. The coefficients, such as those listed in Table I for biofilm phase, are picked up from [1, 2]. In the numerical simulation all coefficients for the boundary layer are assumed to be the same as biofilm phase except the diffusion coefficient B_b^χ that was used in (2.21-2.25). The value of B_b^χ is assumed to be 14 mm^2/day, which is about the one tenth of the diffusion coefficient of active biomass in biofilm phase. Also the diffusion coefficient of limiting substrate, B_O, is varying to achieve different fingering formation. The shear viscosity coefficient $C_\mu = 1.5e-8$ MPa/S and the bulk modulus $C_\kappa = 2.0GPa$ are chosen for water phase whereas $C_\mu = 2.6e-1$ MPa/S and the bulk modulus $C_\kappa = 0.1GPa$ are chosen for biofilm phase and boundary layer. A constant temperature (20^o C) is assumed in the simulations, the isothermal heat capacity C_p for both biofilm and water phase is 4184 Joul/kmg.

Fig. 5 is a comparison of the biofilm thickness growth between 1D theoretical solution in [2] and 2D simulation degenerated to 1D case in this study. Both of them yield each other.

Recall (2.25), it demonstrates that the growth of biofilm globally is governed by the creation of active biomss, i.e. the reaction described by (2.12) for the index $i = 2$. In this case the corresponding coefficients j_2, Λ_{2k}, k=1,2 are given by the second column of Table I. This reaction can be written explicitly as below

$$q_b = m_b Y_{x/o} \frac{m_o}{K_o + m_o} - m_b b \frac{m_o}{K_o + m_o} \tag{5.1}$$

and according to (2.11), when no diffusion and advection:

$$q_b = \dot{m}_b \tag{5.2}$$

in (5.1) and (5.2) m_b and m_o are, respectively, the mess concentrations of the active biomass and limiting substrate; $Y_{x/o}$ is the "Yield of active biomass due to substrate consumption"; b is the "endogenous decay rate coefficient" and $b = 0.2$; K_o is the coefficient of "half-maximum-

rate concentration for utilization of substrate" with the same order as m_o ($K_o = 5e-7 mg/mm^3$). Hence, the second term on the right hand side of (5.1) represents the deaths of bacteria (decay of active biomass), while the first term represents the creation of active biomass through the consumption of limiting substrate. The rate of active biomass creation is mainly controlled by the coefficient $Y_{x/o}$ and monad's law $m_o/(K_o + m_o)$. Displayed in Fig. 6a are the distributions of the volume fraction of active biomass in biofilm phase with varying the coefficient $Y_{x/o}$ after 72 hours growth. From which one sees that smaller $Y_{x/o}$ leads to flat distributions of active biomass with lower amplitudes, which matches the results obtained in [2]. However, when $Y_{x/o}$ is approximately greater than a half, the density of active mess at the middle of biofilm becomes significantly higher than that near the boundary. This is because the middle part of a biofilm has suffered longer reaction than these new growing parts near boundary. According to (5.1-5.2), when $Y_{x/o}$ is significantly greater than *b*, more active biomass will be created after long reaction time. This explanation can be confirmed by the results in Fig. 6b in which the distributions of the density concentration of limiting substrate are plotted corresponding to the cases in Fig. 6a. As expected, larger $Y_{x/o}$ results in a valley of limiting substrate concentration in the middle of biofilm due to the reaction to create new active biomass.

Figs 6a and 6b also verify the conclusion obtained from the fingering formation analysis that the consumption of limiting substrate is the major cause driving biofilm growth. Plotted in Fig. 7 is a simulation of fingering formation of *P. Aeruginosa* biofilm in a water tank with the dimension 2x3 mm where a constant $m_O (= 5.05e-5 mg/mm^3)$ a given at the outer boundary of the domain and an initial value of $m_b (= 1.e-3 mg/mm^3)$ is given within a circle area with the radius 0.01 mm and centered at the middle of the domain. By varying B_O from 344 mm^2/day to 794 mm^2/day, different fingering-shaped biofilm growth have been obtained and are demonstrated in Fig. 7. Fig. 8 is an example of merger process of three pieces of biofilm because it remains as challenge in numerical analysis for simulating the moving boundaries conjunction. The third example is given in Fig.10 with a qualitative comparison with the experimental observation shown in Fig. 9 {Stoodley, 1999 #210}.

6. Conclusions

1) Based on the previous theoretical frameworks in [1, 2, 4], a boundary value problem of biofilm growth has been established associated with a derived generalized Navier-Stokes equations (GNSE) that contains *n+8* (*n+9* for 3D) partial difference equations where *n* the number of active bacteria species.

2) According to mass conservation, an additional constraint has been obtained for the biofilm evolution, which indicates that there is at least one coefficient is predetermined among those coefficients in biofilm kinetics

3) Based on Gibbs equation and generalized Navier-Stokes equation, a thermodynamic framework of biofilm growth has been established which indicates two competing mechanisms which may govern the evolution of biofilm surface. They are: (1) the absorption of nutrition that intends to enlarge the contact area between biofilm and water phase; (2)) the formation of a loose-surface layer that confines a biofilm to accommodate bacteria colonies, which tends to

keep a sphere surface morphology so as to minimize system energy. The quantitative expression of the surface evolution kinetics has been obtained according to the second thermodynamic law. 4) To verify the proposed growth kinetics, two dimensional simulation of biofilm growth has been performed and been compared with experimental observations.

ACKNOWLEDGMENTS:

The first author would like to thank Professor P. Voorhees for the illuminated discussion.

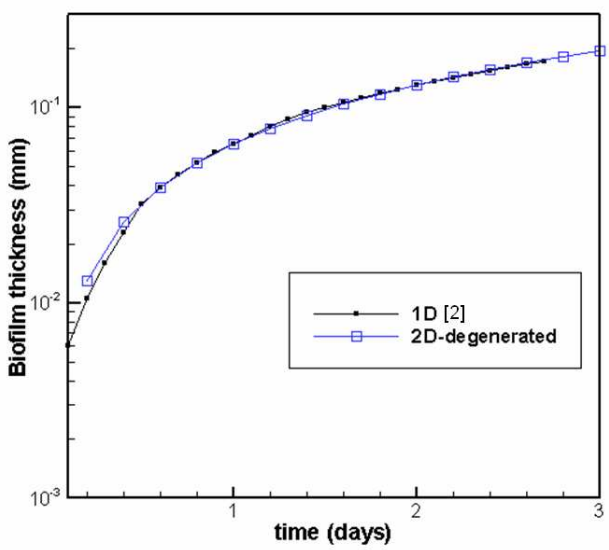

Fig. 5 A comparison of the biofilm thickness growth between 1D theoretical solution in [2] and 2D simulation degenerated to 1D case in this paper

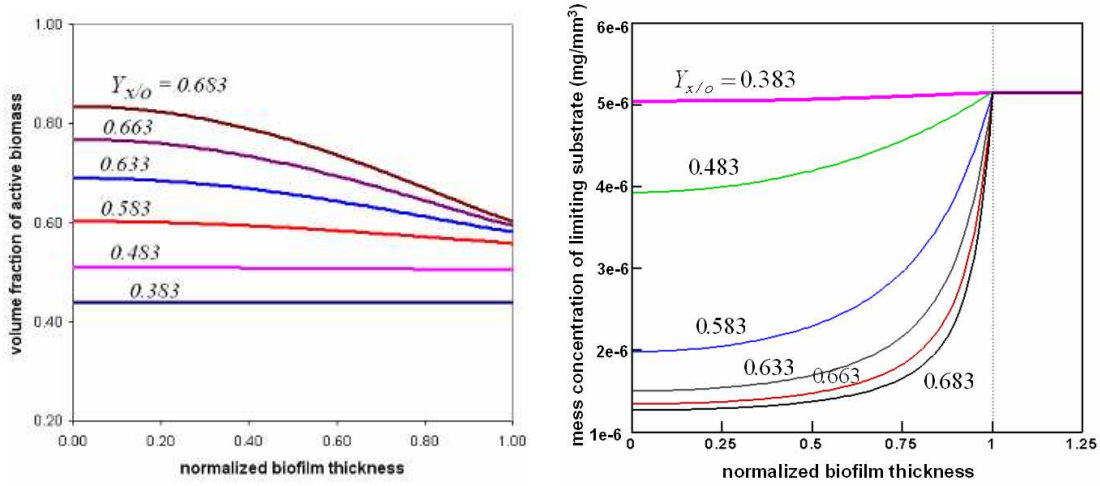

Fig. 6 (a) distributions of volume fraction of active biomass in biofilm with varying $Y_{x/o}$ (b) the corresponding distributions of mess concentration of limiting substrate.

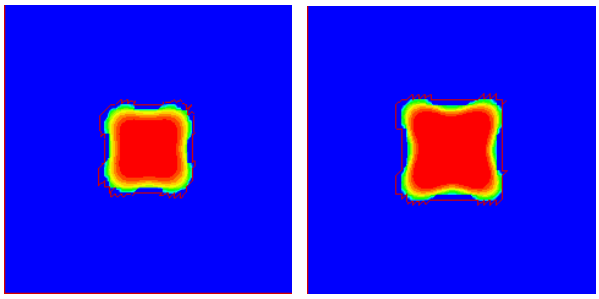

(a) $B_o = 344$ (b) $B_o = 494$

(c) $B_o = 644$ (b) $B_o = 794$

Fig. 7 A simulation of biofilm figuring formation with varying B_O , the diffusion coefficient of limiting substrate, where the unit of B_O is mm^2/day

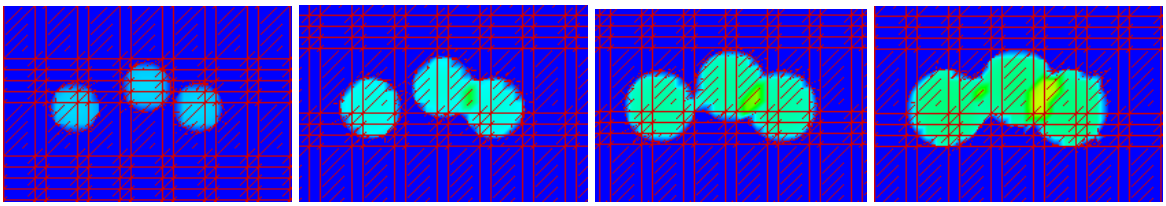

Fig. 8 Snap-shots of the merger of biofilm – conjunction of moving boundaries

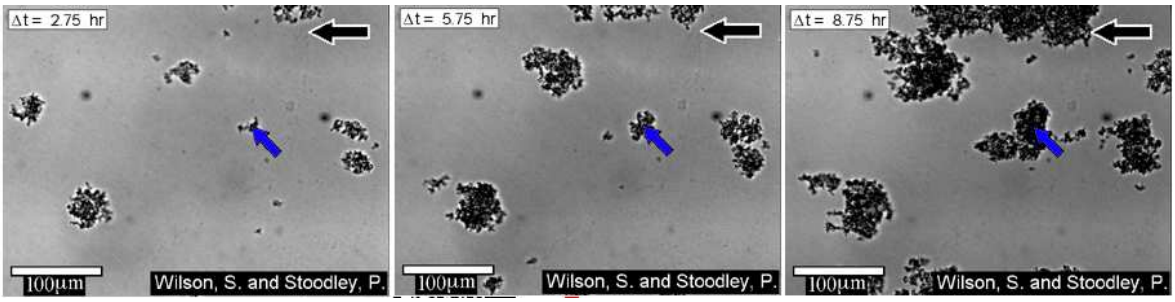

Fig. 9: An experimental observation of the evolution of biofilm [15]; where the arrow at upper-right corner represents the flowing direction and the small arrow new the middle indicates a high concentration of biomass

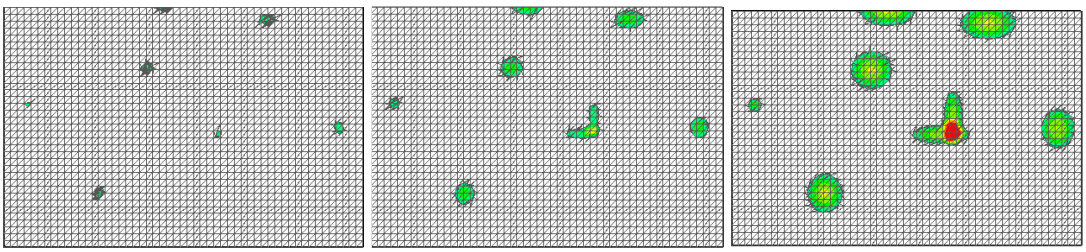

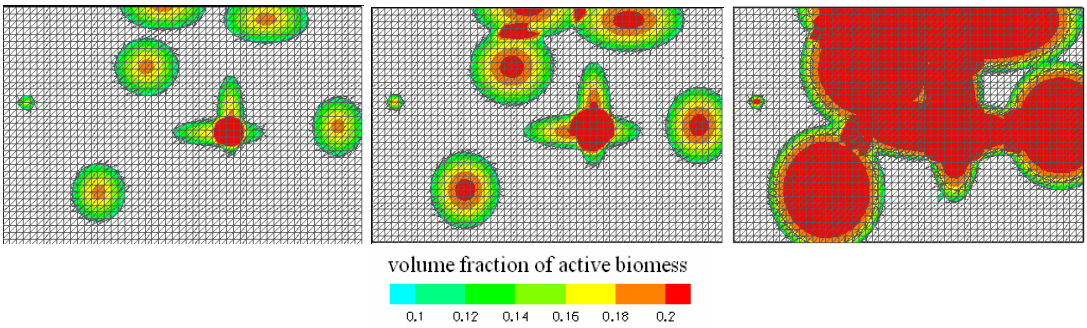

Fig. 10: A simulation of biofilm evolution for the case in Fig. 7; where the contours represent the volume fraction of the active biomass of the "Pseudomonas aeruginosa"; the grey net is the back-ground finite element mesh.

Appendix I

By substituting (3.4) and (3.5) into (2.11) for $\varphi = [e]$ and after some tedious derivations, the energy conservation can be split into the following three independent equations which are engaged for the derivation of (3.6):

$$\frac{\partial}{\partial t}\left(\frac{\rho \boldsymbol{v}\cdot\boldsymbol{v}}{2}\right)+\nabla\cdot\left(\frac{\rho \boldsymbol{v}\cdot\boldsymbol{v}}{2}+\boldsymbol{\sigma}\right)\boldsymbol{v}-\boldsymbol{\sigma}:\nabla\boldsymbol{v}-\sum_k \rho_k \boldsymbol{f}_k\cdot\boldsymbol{v}=0 \qquad \text{(a.1)}$$

$$\frac{\partial}{\partial t}\left(\frac{\rho\Phi}{2}\right)+\nabla\cdot(\rho\Phi\boldsymbol{v})-\sum_k \rho_k \boldsymbol{f}_k\cdot\boldsymbol{v}=0 \qquad \text{(a.2)}$$

$$\frac{\partial \rho u}{\partial t}+\nabla\cdot(\rho u\boldsymbol{v})+\nabla\cdot(\nabla T)+\boldsymbol{\sigma}:\nabla\boldsymbol{v}=0 \qquad \text{(a.3)}$$

Appendix II

As illustrated in Fig. 4, after the transformation $(\mathrm{b})\Rightarrow(\mathrm{a})$ the maximum normal derivation of Γ_b is denoted as δ. By elementary calculation it can be proven that the surface layer length increment $\Delta\Gamma_b$ and the area variation, denoted as ΔS^+ and ΔS^- in Fig. 4, are the same order as δ, i. e.:

$$\Delta\Gamma_b \sim \delta, \qquad S^+ \sim S^- \sim r\delta \qquad \text{(b.1)}$$

where r is the radius of the sphere in Fig. 4b. In the vicinity of the boundary Γ_b, any function can be expressed as a Talyor series:

$$f(\boldsymbol{x}) = f_{\mathrm{T}_b} + \frac{df(\boldsymbol{x})}{d\boldsymbol{x}}\Delta\boldsymbol{x} + \ldots = f_{\mathrm{T}_b} + \frac{df(\boldsymbol{x})}{d\boldsymbol{x}}c_\delta\delta, \qquad 0\le c_\delta \le 1 \qquad \text{(b.2)}$$

where f_{T_b} is the value of $f(\mathbf{x})$ on Γ_b. For an integral of $f(\mathbf{x})$, after the transformation $(\mathrm{b})\Rightarrow(\mathrm{a})$, the difference is

$$F(\delta) = \int_{\Omega_b} [f(x)]_{(b)} d\Omega - \int_{\Omega_b} [f(x)]_{(a)} d\Omega = -\int_{S^+} \left[c_\delta \frac{df(x)}{dx} \delta \right]_{(a)} d\Omega + \int_{S^-} \left[c_\delta \frac{df(x)}{dx} \delta \right]_{(a)} d\Omega \tag{b.3}$$

Applying the mid-value principle of integration and the second relation of (b.1) to (b.3), it can be simplified as

$$F(\delta) = \tilde{c}_\delta r \frac{df(\mathbf{x})}{d\mathbf{x}} \delta^2, \qquad 0 \le \tilde{c}_\delta \le 1 \tag{b.4}$$

So the difference (4.4) for the second term in (4.2) reads

$$-\int_{\Omega_b} \left[\dot{\tilde{s}} - \dot{\chi} \right]_{(b)} d\Omega + \int_{\Omega_b} \left[\dot{\tilde{s}} - \dot{\chi} \right]_{(a)} d\Omega = \frac{\Delta\chi}{\Delta t} \Delta\Gamma_b b_\Gamma + o(\Delta\Gamma_b) \tag{b.5}$$

References

1. Rittmann, B.E., McCarty, P. L., *Environmental Biotechnology*. 2001: McGraw-Hill International Editions.
2. Chopp, D.L., Kirisits, M. J., Moran, B., Parsek, M. R., *The dependence of quorum sensing on the depth of a growth biofilm.* Bulletin of Mathematical Biology, 2003(1): p. 1-34.
3. Watnick, P. and R. Kolter, *Biofilm, city of microbes.* Journal of Bacteriology, 2000. **182**(10): p. 2675-2679.
4. Hall-Stoodley, L., J.W. Costerton, and P. Stoodley, *Bacterial biofilms: From the natural environment to infectious diseases.* Nature Reviews Microbiology, 2004. **2**(2): p. 95-108.
5. Dockery, J. and I. Klapper, *Finger formation in biofilm layers.* Siam Journal on Applied Mathematics, 2002. **62**(3): p. 853-869.
6. Bordas, S., *Extended finite element and level set methods with application to growth of cracks and biofilms*, in *Mech. Engr.* 2003, Northwestern University: Evanston.
7. Cogan, N.G. and J.P. Keener, *The role of the biofilm matrix in structural development.* Mathematical Medicine and Biology-a Journal of the Ima, 2004. **21**(2): p. 147-166.
8. Voorhees, P.W. and M.E. Glicksman, *Analysis of Multiparticle Diffusion.* Journal of Metals, 1982. **35**(12): p. A84-A84.
9. Voorhees, P.W. and M.E. Glicksman, *Solution to the Multi-Particle Diffusion Problem with Applications to Ostwald Ripening .1. Theory.* Acta Metallurgica, 1984. **32**(11): p. 2001-2011.
10. Hughes, T.J.R., L.P. Franca, and M. Mallet, *A New Finite-Element Formulation for Computational Fluid-Dynamics .1. Symmetrical Forms of the Compressible Euler and Navier-Stokes Equations and the 2nd Law of Thermodynamics.* Computer Methods in Applied Mechanics and Engineering, 1986. **54**(2): p. 223-234.
11. Bruce E. Rittmann, P.L.M., *Environmental Biotechnology*. Biological Science Series. 2001: McGraw-Hill.

12. Okabe, S., T. Yasuda, and Y. Watanabe, *Uptake and release of inert fluorescence particles by mixed population biofilms.* Biotechnology and Bioengineering, 1997. **53**(5): p. 459-469.
13. Wirthlin, M.R., G.W. Marshall, and R.W. Rowland, *Formation and decontamination of biofilms in dental unit waterlines.* Journal of Periodontology, 2003. **74**(11): p. 1595-1609.
14. Mullins, W.W., Sekerka, R. F., *Morphological Stability of a Particle Growing by Diffusion or Heat Flow.* J. Appl. Physics, 1963. **34**(2): p. 323.
15. Stoodley, P., Boyle, J. D., DeBeer, D., Lappin-Scott, H. M., *Evolving perspective of biofilm structure.* Biofouling, 1999. **14**(1): p. 75-90.